Application of Two Bayesian Filters to Estimate Unknown Heat Fluxes in a Natural Convection Problem[1]

Marcelo J. Colaço[2]
Mem. ASME
e-mail: colaco@ufrj.br

Helcio R. B. Orlande
e-mail: helcio@mecanica.ufrj.br

Wellington B. da Silva
e-mail: wellingtonuff@yahoo.com.br

Department of Mechanical Engineering,
POLI/COPPE,
Federal University of Rio de Janeiro, UFRJ,
Rio de Janeiro, RJ 21941-972, Brazil

George S. Dulikravich
Fellow ASME
MAIDROC Laboratory, Department of Mechanical and Materials Engineering,
Florida International University,
Miami, FL 33154
e-mail: dulikrav@fiu.edu

Sequential Monte Carlo (SMC) or particle filter methods, which have been originally introduced in the beginning of the 1950s, became very popular in the last few years in the statistical and engineering communities. Such methods have been widely used to deal with sequential Bayesian inference problems in the fields like economics, signal processing, and robotics, among others. SMC methods are an approximation of sequences of probability distributions of interest, using a large set of random samples, named particles. These particles are propagated along time with a simple Sampling Importance distribution. Two advantages of this method are: they do not require the restrictive hypotheses of the Kalman filter, and they can be applied to nonlinear models with non-Gaussian errors. This paper uses two SMC filters, namely the SIR (sampling importance resampling filter) and the ASIR (auxiliary sampling importance resampling filter) to estimate a heat flux on the wall of a square cavity encasing a liquid undergoing natural convection. Measurements, which contain errors, taken at the boundaries of the cavity were used in the estimation process. The mathematical model as well as the initial condition are supposed to have some errors, which were taken into account in the probabilistic evolution model used for the filter. Also, the results using different grid sizes and patterns for the direct and inverse problems were used to avoid the so-called inverse crime. In these results, additional errors were considered due to the different location of the grid points used. The final results were remarkably good when using the ASIR filter. [DOI: 10.1115/1.4006487]

Keywords: particle filter, Bayesian inference, inverse problems, natural convection

Introduction

State estimation problems, also designated *as nonstationary inverse problems* [1], are of great interest in innumerable practical applications. In such kinds of problems, the available measured data are used together with prior knowledge about the physical phenomena and the measuring devices, in order to sequentially produce estimates of the desired dynamic variables. This is accomplished in such a manner that the error is minimized statistically [2]. For example, the position of an aircraft can be estimated through the time-integration of its velocity vector components since departure. However, it may also be measured with a global positioning system (GPS) and an altimeter. State estimation problems deal with the combination of the model prediction (integration of the velocity components that contain errors due to the velocity measurements) and the GPS and altimeter measurements that are also uncertain, in order to obtain more accurate estimations of the system variables (aircraft position).

State estimation problems are solved with the so-called Bayesian filters [1,2]. In the Bayesian approach to statistics, an attempt is made to utilize all available information in order to reduce the amount of uncertainty present in an inferential or decision-making problem. As new information is obtained, it is combined with previous information to form the basis for statistical procedures. The formal mechanism used to combine the new information with the previously available information is known as Bayes' theorem [1,3].

The most widely known Bayesian filter method is the Kalman filter [1,2,4–9]. However, the application of the Kalman filter is limited to linear models with additive Gaussian noises. Extensions of the Kalman filter were developed in the past for less restrictive cases by using linearization techniques [1,3,6–8]. Similarly, Monte Carlo methods have been developed in order to represent the posterior density in terms of random samples and associated weights. Such Monte Carlo methods, usually denoted as particle filters among other designations found in the literature, do not require the restrictive hypotheses of the Kalman filter. Hence, particle filters can be applied to nonlinear models with non-Gaussian errors [1,4,8–17].

Hammersley and Hanscomb [18] presented a technique that used recursive Bayesian filters, together with Monte Carlo simulations, known as sequential importance sampling (SIS). In this approach, the key idea was to represent the posterior probability function as a set of random samples associated with some weights, in order to calculate the estimates based on such samples and weights. Gordon et al. [19] added an extra step, named resampling, into the SIS method to avoid the problem known as degeneration of particles. This filter is known as SIR filter. In 2008, Orlande et al. [20] presented an application of the SIR filter to a nonlinear heat conduction problem.

In order to overcome some difficulties of SIR filter, Pitt and Shephard [21] introduced the auxiliary particle filter (APF). In 2006, Del Moral et al. [16] presented an alternative to improve the SIR filter, named sequential Monte Carlo samplers, introducing a method for the evolution of the particles and also an artificial delayed kernel.

[1]A shorter version of this paper was awarded as the Best Paper by the 2011 Advanced Modeling and Simulation Technical Committee at ASME 2011 International Design Engineering Technical Conferences & Computers and Information in Engineering Conference, IDETC/CIE 2011, August 29–31, 2011, Washington, DC.

[2]Corresponding author.

Contributed by the Heat Transfer Division of ASME for publication in the JOURNAL OF HEAT TRANSFER. Manuscript received September 27, 2011; final manuscript received March 22, 2012; published online July 9, 2012. Assoc. Editor: Oronzio Manca.

Another well-known filter is the combined parameter and state estimation in simulation-based filtering, proposed by Liu and West [22], which uses a combination of the artificial evolution method (where the problem related with the loss of information is avoided) and the smoothness kernel proposed by West [23], which improves the choice of the particles. In 2007, Sisson et al. [24] presented a new filter technique, where the sequential Monte Carlo method was coupled with the approximate Bayesian computation, named sequential Monte Carlo without likelihoods.

In this paper, the SIR and the ASIR algorithms were applied to estimate an unknown heat flux at a top wall of a square cavity undergoing a natural thermal convection process. Two different heat flux profiles were estimated with very good results. Also, the influence of the number of particles used as well as the frequency of the measurements were analyzed.

Physical Problem

The physical problem under consideration in this paper involves the transient laminar natural convection of a fluid inside a two-dimensional square cavity. The fluid is initially at rest and at the uniform temperature, T_c. At time zero, the bottom and top surfaces are subjected to time-dependent heat fluxes $q_1(t)$ and $q_2(t)$, respectively. The left and right surfaces are subjected to constant temperatures T_c and T_h, respectively. The fluid properties are assumed constant, except for the density in the thermal buoyancy term, where we consider Boussinesq's approximation valid [25].

The mathematical formulation for this physical problem can be written in vector form in terms of the following conservation equation in Cartesian coordinates:

$$\frac{\partial(\rho\boldsymbol{\varphi})}{\partial t}+\frac{\partial(u\rho\boldsymbol{\varphi})}{\partial x}+\frac{\partial(v\rho\boldsymbol{\varphi})}{\partial y}=\nabla\bullet\left(\boldsymbol{\Gamma}^{\phi}\bullet\nabla\boldsymbol{\varphi}\right)+\mathbf{S}^{\phi} \tag{1}$$

The general conservation variable as well as the diffusion coefficient and the source term for the mass, momentum, and energy conservation equations are given in vector form, respectively, as

$$\boldsymbol{\Gamma}^{\phi}=\begin{bmatrix}0&0&0&0\\0&\mu&0&0\\0&0&\mu&0\\0&0&0&\dfrac{k}{C_P}\end{bmatrix} \tag{2a}$$

$$\boldsymbol{\varphi}=\begin{bmatrix}1\\u(x,y,t)\\v(x,y,t)\\T(x,y,t)\end{bmatrix} \tag{2b}$$

$$\mathbf{S}^{\phi}=\begin{bmatrix}0\\-\dfrac{\partial p(x,y,t)}{\partial x}\\-\dfrac{\partial p(x,y,t)}{\partial y}-\rho g\{1-\beta[T(x,y,t)-T_{\mathrm{ref}}]\}\\0\end{bmatrix} \tag{2c}$$

We note in the Eq. (2c) that the positive y-axis in the physical domain is supposed to be aligned with the opposite direction of the gravitational acceleration vector. These equations are solved, subject to the following boundary and initial conditions:

$$T=T_c \quad \text{at} \quad x=1, 1<y<H, \ \text{for}\ t>0 \tag{3a}$$

$$T=T_h \quad \text{at} \quad x=W, 1<y<H, \ \text{for}\ t>0 \tag{3b}$$

$$u=v=0 \quad \text{at} \quad x=1 \quad \text{and} \quad x=W, 1<y<H, \ \text{for}\ t>0 \tag{3c}$$

$$u=v=0 \quad \text{at} \quad y=1 \quad \text{and} \quad y=H, 1<x<W, \ \text{for}\ t>0 \tag{3d}$$

$$k\frac{\partial T}{\partial y}=-q_1(t) \quad \text{at} \quad y=1, 1<x<W, \ \text{for}\ t>0 \tag{3e}$$

$$k\frac{\partial T}{\partial y}=q_2(t) \quad \text{at} \quad y=H, 1<x<W, \ \text{for}\ t>0 \tag{3f}$$

$$u=v=0 \quad \text{for} \quad t=0 \ \text{in the region} \tag{3g}$$

$$T=T_c \quad \text{for} \quad t=0 \ \text{in the region} \tag{3h}$$

The above equations were transformed from the physical Cartesian (x,y) coordinates to the computational coordinate system (ξ,η) and solved by the finite volume method [26]. The SIMPLEC (semi-implicit method for pressure-linked equations, consistent) method [27] was used to solve the velocity-pressure coupling problem. The weighted upstream differencing scheme (WUDS) interpolation scheme [28] was used to obtain the values of u, v, and T as well as their derivatives at the interfaces of each control volume. The resulting linear system was solved by the GMRES (generalized minimal residual) method [29]. For details on the solution procedure, as well as the verification of the code against results published in the literature, the reader is advised to consult Refs. [30–37].

Inverse Problem

The solution of the inverse problem within the Bayesian framework is recast in the form of statistical inference from the *posterior probability density*, which is the model for the conditional probability distribution of the unknown parameters given the measurements. The measurement model incorporating the related uncertainties is called the *likelihood*, that is, the conditional probability of the measurements given the unknown parameters. By assuming that the measurement errors are Gaussian random variables, with zero means and known covariance matrix $\mathbf{W}$ and that the measurement errors are additive and independent of the parameters $\mathbf{P}$, the *likelihood function* can be expressed as [1,3,38–42]

$$\pi(\mathbf{Y}|\mathbf{P})=(2\pi)^{-D/2}|\mathbf{W}|^{-1/2}\exp\left\{-\frac{1}{2}[\mathbf{Y}-\mathbf{T}(\mathbf{P})]^{T}\mathbf{W}^{-1}[\mathbf{Y}-\mathbf{T}(\mathbf{P})]\right\} \tag{4}$$

where $\mathbf{Y}$ is the measurements and $\mathbf{T}(\mathbf{P})$ is the solution of the direct (forward) problem. Such solution is obtained from the mathematical formulation of the heat transfer problem under analysis with known $\mathbf{P}$.

The model for the unknowns that reflects all the uncertainty of the parameters without the information conveyed by the measurements is called the *prior* model [1,3,38–42].

The formal mechanism to combine the new information (measurements) with the previously available information (prior) is known as the Bayes' theorem [1,3,38–42]. Therefore, the term Bayesian is often used to describe the statistical inversion approach, which is based on the following principles [1]:

(1) All variables included in the model are modeled as random variables.
(2) The randomness describes the degree of information concerning their realizations.
(3) The degree of information concerning these values is coded in probability distributions.
(4) The solution of the inverse problem is the posterior probability distribution, from which distribution point estimates and other statistics are computed. Therefore, this approach relies fundamentally on the principles of the Bayesian statistics to obtain the solution of inverse problems. Recent works on the application of Bayesian techniques to inverse heat transfer problems include Refs. [43–56].

Bayes' theorem is stated as [1,3,38–42]

$$\pi_{\mathrm{posterior}}(\mathbf{P})=\pi(\mathbf{P}|\mathbf{Y})=\frac{\pi(\mathbf{P})\pi(\mathbf{Y}|\mathbf{P})}{\pi(\mathbf{Y})} \tag{5}$$

where $\pi_{\mathrm{posterior}}(\mathbf{P})$ is the posterior probability density, $\pi(\mathbf{P})$ is the prior density, $\pi(\mathbf{Y}|\mathbf{P})$ is the likelihood function, and $\pi(\mathbf{Y})$ is the

marginal probability density of the measurements, which plays the role of a normalizing constant.

State Estimation

State estimation problems, also designated as nonstationary inverse problems [1], are of great interest in innumerable practical applications. In such kinds of problems, the available measured data are used together with prior knowledge about the physical phenomena and the measuring devices, in order to sequentially produce estimates of the desired dynamic variables. This is accomplished in such a manner that the error is minimized statistically [2].

Consider a model for the evolution of the state variables $\mathbf{x}$ in the form

$$\mathbf{x}_k = \mathbf{f}_k(\mathbf{x}_{k-1}, \mathbf{v}_k) \tag{6}$$

where $\mathbf{f}$ is, in the general case, a nonlinear function of $\mathbf{x}$ and of the state noise or uncertainty vector given by $\mathbf{v}_k \in \mathbf{R}^{\mathbf{n}}$. The vector $\mathbf{x}_k \in \mathbf{R}^{\mathbf{n}}$ is called the state vector and contains the variables to be dynamically estimated. This vector advances in time in accordance with the *state evolution model* (6). The subscript $k = 1, 2, 3, \ldots$, denotes a time instant t_k in a dynamic problem.

The observation model describes the dependence between the state variable $\mathbf{x}$ to be estimated and the measurements $\mathbf{z}$ through the general, possibly nonlinear, function $\mathbf{h}$. This can be represented by

$$\mathbf{z}_k = \mathbf{h}_k(\mathbf{x}_k, \mathbf{n}_k) \tag{7}$$

where $\mathbf{z}_k \in \mathbf{R}^{\mathbf{n}z}$ are available at times t_k, $k = 1, 2, 3, \ldots$. Equation (7) is referred to as the *observation/measurement model*. The vector $\mathbf{n}_k \in \mathbf{R}^{\mathbf{n}z}$ represents the measurement noise or uncertainty.

As per Eqs. (6) and (7), the *evolution and observation models* are based on the following assumptions [1,2,4–9,56]:

(a) The sequence $\mathbf{x}_k$ for $k = 1, 2, 3, \ldots$, is a Markovian process, that is

$$\pi(\mathbf{x}_k|\mathbf{x}_0, \mathbf{x}_1, \ldots, \mathbf{x}_{k-1}) = \pi(\mathbf{x}_k|\mathbf{x}_{k-1}) \tag{8a}$$

(b) The sequence $\mathbf{z}_k$ for $k = 1, 2, 3, \ldots$, is a Markovian process with respect to the history of $\mathbf{x}_k$, that is

$$\pi(\mathbf{z}_k|\mathbf{x}_0, \mathbf{x}_1, \ldots, \mathbf{x}_k) = \pi(\mathbf{z}_k|\mathbf{x}_k) \tag{8b}$$

(c) The sequence $\mathbf{x}_k$ depends on the past observations only through its own history, that is

$$\pi(\mathbf{x}_k|\mathbf{x}_{k-1}, \mathbf{z}_1, \mathbf{z}_2, \ldots, \mathbf{z}_{k-1}) = \pi(\mathbf{x}_k|\mathbf{x}_{k-1}) \tag{8c}$$

where $\pi(\mathbf{a}|\mathbf{b})$ denotes the conditional probability of $\mathbf{a}$ when $\mathbf{b}$ is given.

For the state and observation noises, the following assumptions are made [1,2,4–9,56]:

(a) For $i \neq j$, the noise vectors $\mathbf{v}_i$ and $\mathbf{v}_j$, as well as $\mathbf{n}_i$ and $\mathbf{n}_j$, are mutually independent and also mutually independent of the initial state $\mathbf{x}_0$.

(b) The noise vectors $\mathbf{v}_i$ and $\mathbf{n}_j$ are mutually independent for all i and j.

Different problems can be considered for the evolution-observation models described above, such as [1,2,4–9,56]

(i) The *prediction problem*, when the objective is to obtain $\pi(\mathbf{x}_k|\mathbf{z}_{1:k-1})$.

(ii) The *filtering problem*, when the objective is to obtain $\pi(\mathbf{x}_k|\mathbf{z}_{1:k})$.

(iii) The *fixed-lag smoothing problem*, when the objective is to obtain $\pi(\mathbf{x}_k|\mathbf{z}_{1:k+p})$, where $p \geq 1$ is the fixed lag.

(iv) The *whole-domain smoothing problem*, when the objective is to obtain $\pi(\mathbf{x}_k|\mathbf{z}_{1:K})$, where $\mathbf{z}_{1:K} = \{\mathbf{z}_i, i = 1, \ldots, K\}$ is the complete set of measurements.

We consider here the filtering problem. By assuming that $\pi(\mathbf{x}_0|\mathbf{z}_0) = \pi(\mathbf{x}_0)$ is available, the posterior probability density $\pi(\mathbf{x}_k|\mathbf{z}_{1:k})$ is then obtained with Bayesian filters in two steps [1,2,4–9]: *prediction* and *update*, as illustrated in Fig. 1.

The most widely known Bayesian filter method is the Kalman filter [1,2,4–17,20,56–58]. However, the application of the Kalman filter is limited to linear models with additive Gaussian noises. Extensions of the Kalman filter were developed in the past for less restrictive cases by using linearization techniques. Similarly, Monte Carlo methods have been developed in order to represent the posterior density in terms of random samples and associated weights. Such Monte Carlo methods, usually denoted as particle filters among other designations found in the literature, do not require the restrictive hypotheses of the Kalman filter. Hence, particle filters can be applied to nonlinear models with non-Gaussian errors [1,2,4–17,20,57,58].

The main idea in the particle filter is to represent the required posterior density function by a set of random samples with associated weights and to compute the estimates based on these samples and weights [1,8–17,20,57,58]. Let $\{\mathbf{x}^i_{0:k}, i = 0, \ldots, N\}$ be the particles with associated weights $\{\mathbf{w}^i_k, i = 0, \ldots, N\}$ and $\mathbf{x}_{0:k} = \{\mathbf{x}_j, j = 0, \ldots, k\}$ be the set of all states up to t_k, where N is the number of particles. The weights are normalized, so that $\sum_i w^i_k = 1$. Then, the posterior density at t_k can be discretely approximated by

$$\pi(\mathbf{x}_{0:k}|\mathbf{z}_{1:k}) \approx \sum_{i=1}^{N} w^i_k \, \delta(\mathbf{x}_{0:k} - \mathbf{x}^i_{0:k}) \tag{9}$$

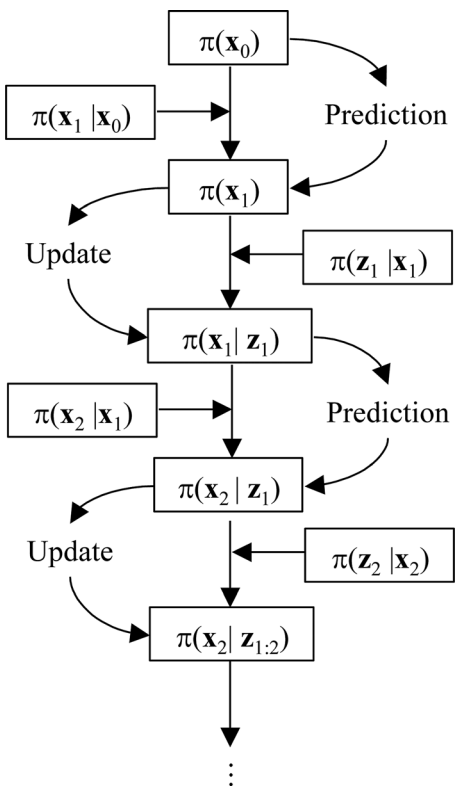

Fig. 1 Prediction and update steps [1]

Table 1 SIR algorithm [8,9]

Step 1
For $i = 1, \ldots, N$, draw new particles $\mathbf{x}_k^i$ from the prior density $\pi(\mathbf{x}_k|\mathbf{x}_{k-1}^i)$ and then use the likelihood density to calculate the correspondent weights $w_k^i = \pi(\mathbf{z}_k|\mathbf{x}_k^i)$
Step 2
Calculate the total weight $t = \sum_i w_k^i$ and then normalize the particle weights, that is, for $i = 1, \ldots, N$ let $w_k^i = t^{-1} w_k^i$
Step 3
Resample the particles as follows:
Construct the cumulative sum of weights (CSW) by computing $c_i = c_{i-1} + w_k^i$ for $i = 1, \ldots, N$, with $c_0 = 0$
Let $i = 1$ and draw a starting point u_1 from the uniform distribution U[0,N^{-1}]
For $j = 1, \ldots, N$
  Move along the CSW by making $u_j = u_1 + N^{-1}(j-1)$
  While $u_j > c_i$ make $i = i+1$
  Assign sample $x_k^j = x_k^i$
  Assign sample $w_k^j = N^{-1}$

where $\delta(.)$ is the Dirac delta function. Similarly, its marginal distribution, which is of interest for the filtering problem, can be approximated by $\pi(\mathbf{x}_k|\mathbf{z}_{1:k}) \approx \sum_{i=1}^{N} w_k^i \, \delta(\mathbf{x}_k - \mathbf{x}_k^i)$.

A common problem with the particle filter method is the degeneracy phenomenon, where after a few states all but one particle may have negligible weight. The degeneracy implies that a large computational effort is devoted to updating particles whose contribution to the approximation of the posterior density function is almost zero. This problem can be overcome by increasing the number of particles. In addition, the use of the resampling technique is recommended to avoid the degeneracy of the particles [1,8–17,20,57,58].

Resampling generally involves a mapping of the random measure $\{\mathbf{x}_k^i, w_k^i\}$ into a random measure $\{\mathbf{x}_k^{i*}, N^{-1}\}$ with uniform weights. It can be performed if the number of effective particles with large weights falls below a certain threshold number. Alternatively, resampling can also be applied indistinctively at every instant t_k, as in the SIR algorithm [8,9]. This algorithm can be summarized in the steps presented in Table 1, as applied to the system evolution from t_{k-1} to t_k.

Although the resampling step reduces the effects of the degeneracy problem, it may lead to a loss of diversity and the resultant sample can contain many repeated particles. This problem, known as sample impoverishment, can be severe in the case of small evolution model noise. In this case, all particles collapse to a single particle within few instants t_k. Another drawback of the particle filter is related to the large computational cost due to the Monte Carlo method, which may limit its application only to fast computing problems. Different algorithms for the implementation of the particle filter can be found in Ref. [58], including those that permit the simultaneous estimation of constant parameters appearing in the model and the transient states.

In addition, in the SIR algorithm the state space is explored without the information conveyed by the measurements, that is, the particles at each time instant are generated through the sole application of the transition prior $\pi(\mathbf{x}_k^i|\mathbf{x}_{k-1}^i)$ (see step 1 in Table 1). With the ASIR algorithm an attempt is made to overcome these drawbacks, by performing the resampling step at time t_{k-1}, with the available measurement at time t_k [9]. The resampling is based on some point estimate ν_k^i that characterizes $\pi(\mathbf{x}_k|\mathbf{x}_{k-1}^i)$, which can be the mean of $\pi(\mathbf{x}_k|\mathbf{x}_{k-1}^i)$ or simply a sample of $\pi(\mathbf{x}_k|\mathbf{x}_{k-1}^i)$. If the state evolution model noise is small, $\pi(\mathbf{x}_k|\mathbf{x}_{k-1}^i)$ is generally well characterized by ν_k^i, so that the weights w_k^i are more even and the ASIR algorithm is less sensitive to outliers than the SIR algorithm. On the other hand, if the state evolution model noise is large, the single point estimate ν_k^i in the state space may not characterize well $\pi(\mathbf{x}_k|\mathbf{x}_{k-1}^i)$ and the ASIR algorithm may not be as effective as the SIR algorithm. The ASIR algorithm can be summarized in the steps presented in Table 2, as applied to the system evolution from t_{k-1} to t_k [8,9]. According to Ref. [8], the advantage of the ASIR filter over the SIR algorithm is that it naturally generates points from the sample at $k-1$, which, conditioned on the current measurement, are most likely to be close to the true state. Yet as described in Ref. [8], ASIR can be viewed as resampling at the previous time step, based on some point estimates ν_k^i that characterize $\pi(\mathbf{x}_k|\mathbf{x}_{k-1}^i)$.

Results and Discussions

In this paper, we applied the SIR and ASIR filters to estimate a time-varying heat flux applied to the top wall of a square cavity filled with air ($\rho = 1.19\,\mathrm{kg\,m^{-3}}$, $k = 0.02624\,\mathrm{W\,m^{-1}\,K^{-1}}$, $C_p = 1035.0222\,\mathrm{J\,kg^{-1}\,K^{-1}}$, $\mu = 1.8 \times 10^{-5}\,\mathrm{kg\,m^{-1}\,s^{-1}}$, $\beta = 0.00341\,\mathrm{K^{-1}}$).

Table 2 ASIR algorithm [8,9]

Step 1
For $i = 1, \ldots, N$, draw new particles $\mathbf{x}_k^i$ from the prior density $\pi(\mathbf{x}_k|\mathbf{x}_{k-1}^i)$ and then calculate some characterization of $\mathbf{x}_k$, given $\mathbf{x}_{k-1}^i$, as for example the mean $\nu_k^i = \mathrm{E}[\mathbf{x}_k|\mathbf{x}_{k-1}^i]$. Then, use the likelihood density to calculate the correspondent weights $w_k^i = \pi(\mathbf{z}_k|\nu_k^i) w_{k-1}^i$
Step 2
Calculate the total weight $t = \sum_i w_k^i$ and then normalize the particle weights, that is, for $i = 1, \ldots, N$ let $w_k^i = t^{-1} w_k^i$
Step 3
Resample the particles as follows:
Construct the CSW by computing $c_i = c_{i-1} + w_k^i$ for $i = 1, \ldots, N$, with $c_0 = 0$
Let $i = 1$and draw a starting point u_1 from the uniform distribution U[0,N^{-1}]
For $j = 1, \ldots, N$
  Move along the CSW by making $u_j = u_1 + N^{-1}(j-1)$
  While $u_j > c_i$ make $i = i+1$
  Assign sample $x_k^j = x_k^i$
  Assign sample $w_k^j = N^{-1}$
  Assign parent $i^j = i$
Step 4
For $j = 1, \ldots, N$, draw particles $\mathbf{x}_k^j$ from the prior density $\pi(\mathbf{x}_k|\mathbf{x}_{k-1}^{ij})$, using the parent i^j, and then use the likelihood density to calculate the correspondent weights $w_k^j = \pi(\mathbf{z}_k|\mathbf{x}_k^j)/\pi(\mathbf{z}_k|\mathbf{v}_k^{ij})$
Step 5
Calculate the total weight $t = \sum_j w_k^j$ and then normalize the particle weights, that is, for $j = 1, \ldots, N$ let $w^j{}_k = t^{-1} w^j{}_k$

Table 3 Test cases analyzed

Case	Heat flux	Particles	Frequency	Grid size for the generation of measurements	Grid size for the inverse problem
1	$q_2(t) = 0.01t$ (W m^{-2})	10	1 Hz	11×11	
2			10 Hz		
3		100	1 Hz		
4			10 Hz		
5		10	1 Hz		
6			10 Hz		
7		100	1 Hz		
8	$q_2(t) = 0$ W m^{-2} for $t < 500$ s		10 Hz		
9	$q_2(t) = 5$ W m^{-2} for $t > 500$ s	10	1 Hz	111×111	21×21
10			10 Hz		
11		100	1 Hz		
12			10 Hz		

The bottom wall of the cavity was kept thermally insulated and the left and right walls were subjected to constant temperatures equal to 2 °C and 12 °C, respectively. The width and height of the cavity were equal to 0.045841 m, which resulted in a Rayleigh (Ra) number equal to 10^5, where

$$\mathrm{Ra} = \frac{\rho^2 C_p g \beta (T_h - T_c) H^3}{\mu k} \tag{10}$$

The state estimation problem consists thus in predicting the behavior of the state variable $q_2(t)$ at the top wall of the cavity. However, since the heat flux affects the temperature field through the energy equation and also the mass and momentum equations through the buoyancy source term, Eqs. (1)–(3), the state vector $\mathbf{x}$ appearing in Eq. (6) is composed of the discrete heat flux $q_2(t)$ at each time step, plus all velocity components and temperature at each finite volume inside the cavity. Due to the excessive amount of computational resources required for the solution of this problem, in the first part of this paper we used a very coarse finite volume grid (10×10 volumes) both to the generation of the simulated measurements and to the solution of the inverse problem, in order to compare the two particle filters (SIR and ASIR) used in this work. At the end of this paper, in order to avoid the so-called inverse crime, a grid with 110×110 volumes was used in the direct problem and a grid with 20×20 volumes was used in the inverse problem. The use of different grid sizes for the direct and inverse problems also introduces additional errors, since the location of the measurement points is not the same for the two grids used. More details on this will be addressed below.

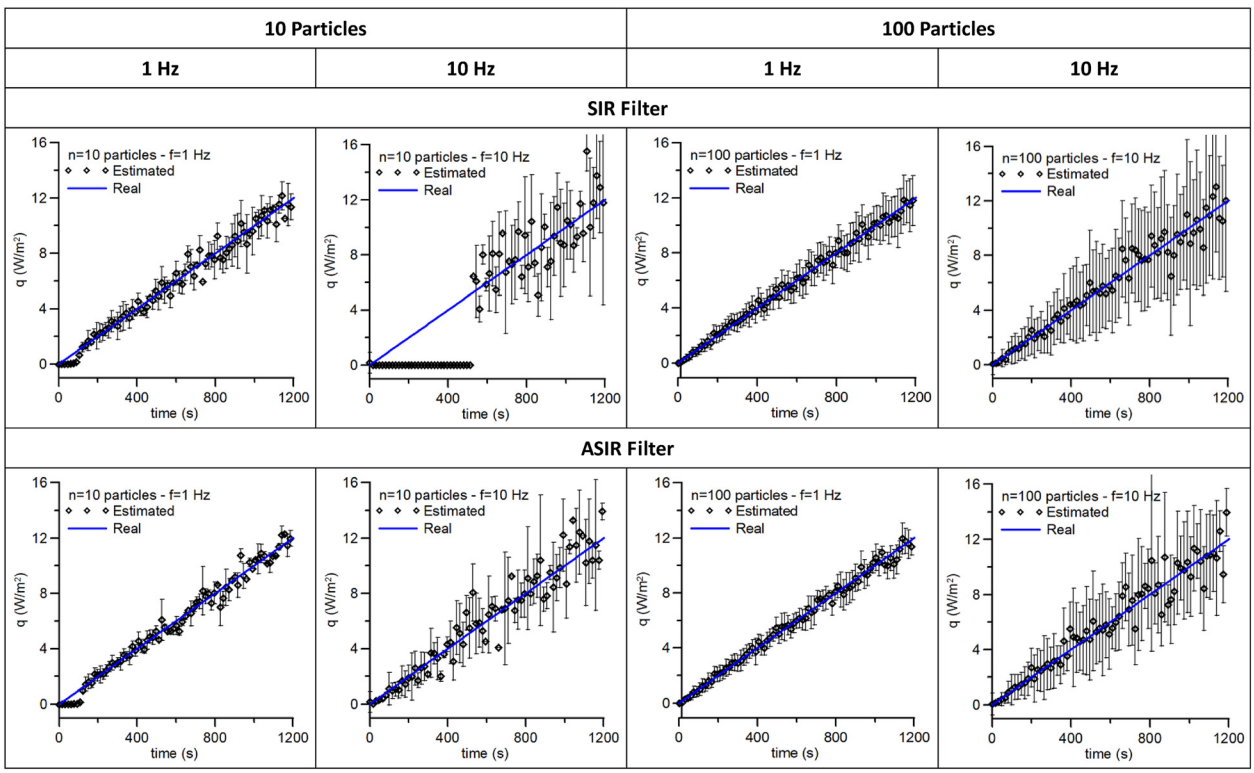

Fig. 2 Estimated heat flux with the linear profile

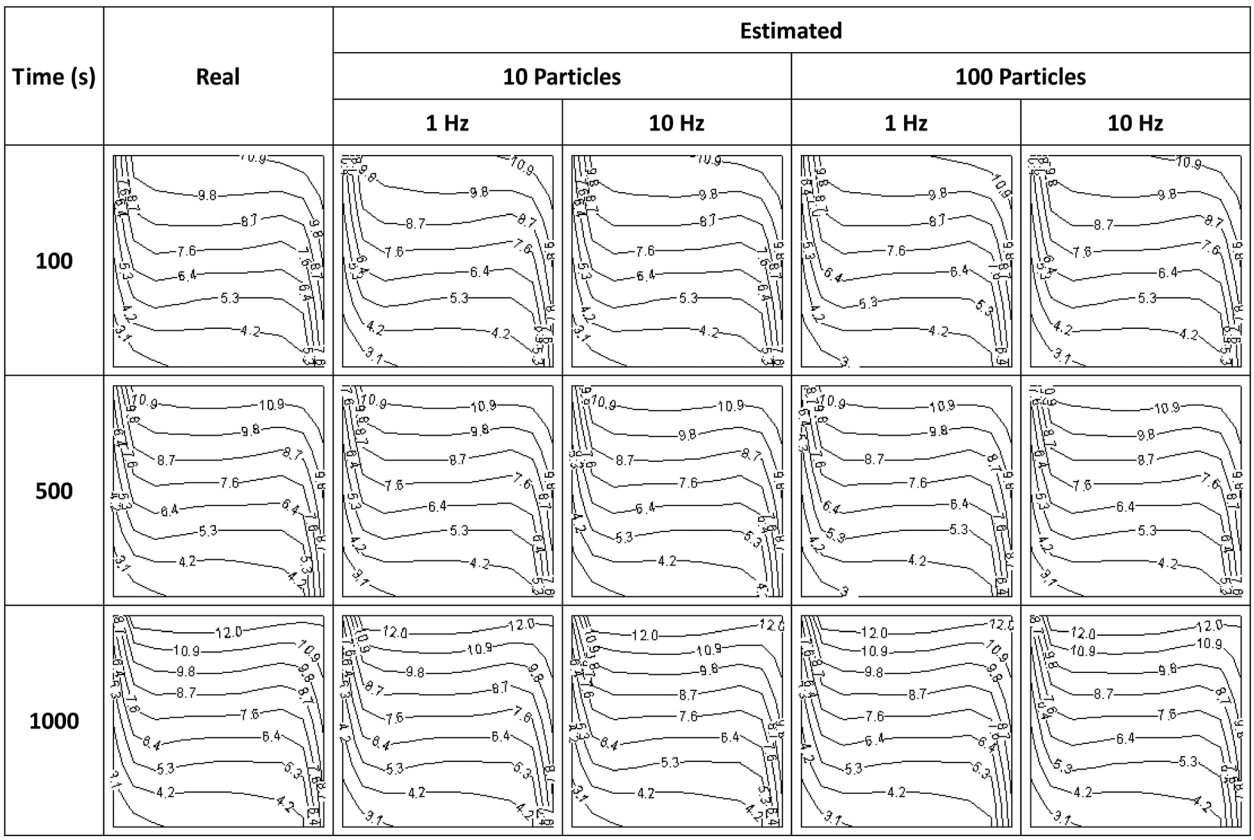

Fig. 3 Real and estimated temperature profiles with the linear heat flux profile (ASIR filter)

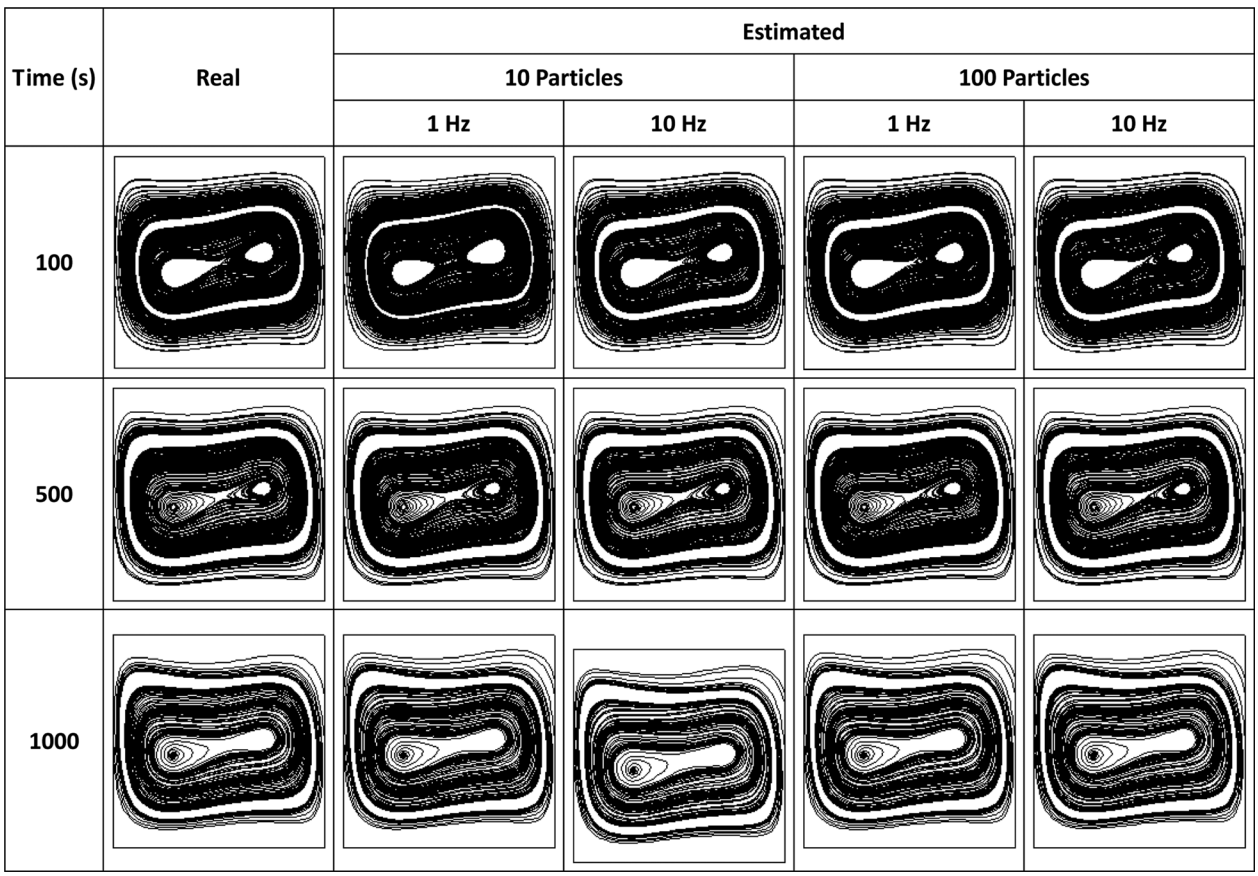

Fig. 4 Real and estimated streamlines with the linear heat flux profile (ASIR filter)

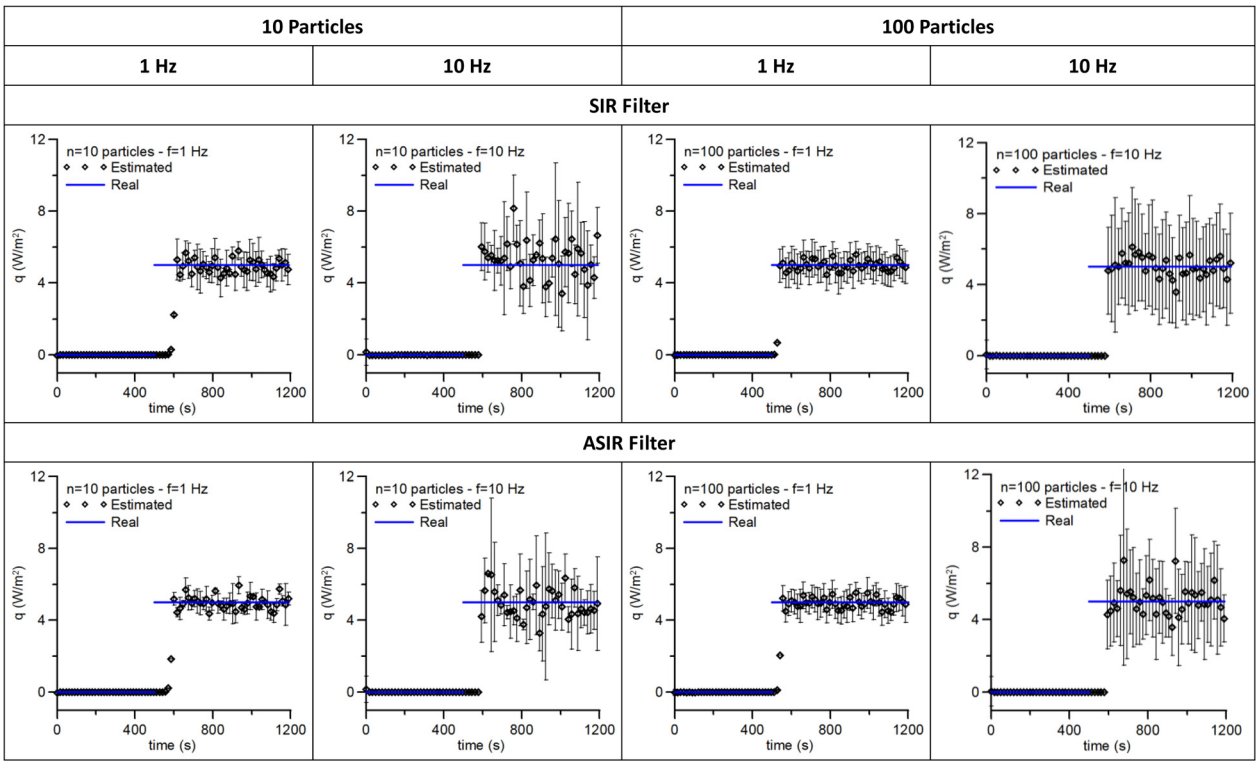

Fig. 5 Estimated heat flux with the step profile

The total number of state variables for the grid with 10×10 volumes are thus 1 for the heat flux $q_2(t)$, 11×11 for the u component of the velocity field, 11×11 for the v component of the velocity field, and 11×11 for the temperature T, resulting in 364 state variables. For the case with 20×20 volumes, the total number of state variables was 1324. Thus, different sizes of the state variable vectors were also compared in this paper.

In the framework of the particle filters, two auxiliary models are needed: (i) an evolution model, given by Eq. (6); and (ii) an observation model, given by Eq. (7). For the evolution model, we used two submodels: (i.i) an evolution model for the velocity and temperature fields, given by the discretization of mass, momentum, and energy equations, Eqs. (1)–(3), where the state noise $\mathbf{v}$, appearing in Eq. (6), was supposed to be equal 1% of the state variable values, that is

$$\mathbf{x}_k = \mathbf{x}_k + \sigma\varepsilon \Rightarrow \begin{array}{r} u(t) = u(t)[1 + 0.01\varepsilon] \\ v(t) = v(t)[1 + 0.01\varepsilon] \\ T(t) = T(t)[1 + 0.01\varepsilon] \end{array} \tag{11}$$

where ε is a random variable with Gaussian distribution and zero mean; and (i.ii) an evolution model for the heat flux $q_2(t)$ which was taken as a random walk model

$$q_2(t) = q_2(t - \Delta t) + \sigma_q \varepsilon \tag{12}$$

where σ_q varied automatically between 10% and 100% of the value of $q_2(t - \Delta t)$. Such variation was based on the likelihood of all particles. If the likelihood function was equal to zero for all particles, then σ_q was increased in intervals of 10% for the next time steps until at least one of the particles had a non-null value of the likelihood function. Then, σ_q was reduced again in intervals of 10% for the next time steps.

For the observation model, we used simulated temperature measurements, where an experimental error with standard deviation equal to 1% of the local value of the temperature was used. Such measurements were taken at the top and bottom walls of the cavity at 11 points equally spaced at each wall for the grid with 11×11 points and at 21 points equally spaced at each wall for the grid with 21×21 points.

Two different profiles were tried for the heat flux $q_2(t)$. Also, two different numbers of particles and two frequencies of observations were analyzed. Table 3 summarizes the test cases

Table 4 Location of the sensors for the direct and inverse problems for test cases 9–12

Direct problem (x)	Inverse problem (x)	Error %
0.00103246	0.00109145	5.7
0.00309736	0.00327436	5.7
0.00516227	0.00545726	5.7
0.00764017	0.00764017	0.0
0.00970508	0.00982307	1.2
0.01177	0.012006	2.0
0.0138349	0.0141889	2.6
0.0163128	0.0163718	0.4
0.0183777	0.0185547	1.0
0.0204426	0.0207376	1.4
0.0225075	0.0229205	1.8
0.0249854	0.0251034	0.5
0.0270503	0.0272863	0.9
0.0291152	0.0294692	1.2
0.0315931	0.0316521	0.2
0.033658	0.033835	0.5
0.0357229	0.0360179	0.8
0.0377879	0.0382008	1.1
0.0402657	0.0403837	0.3
0.0423307	0.0425666	0.6
0.0443956	0.0447495	0.8
Average error		1.6

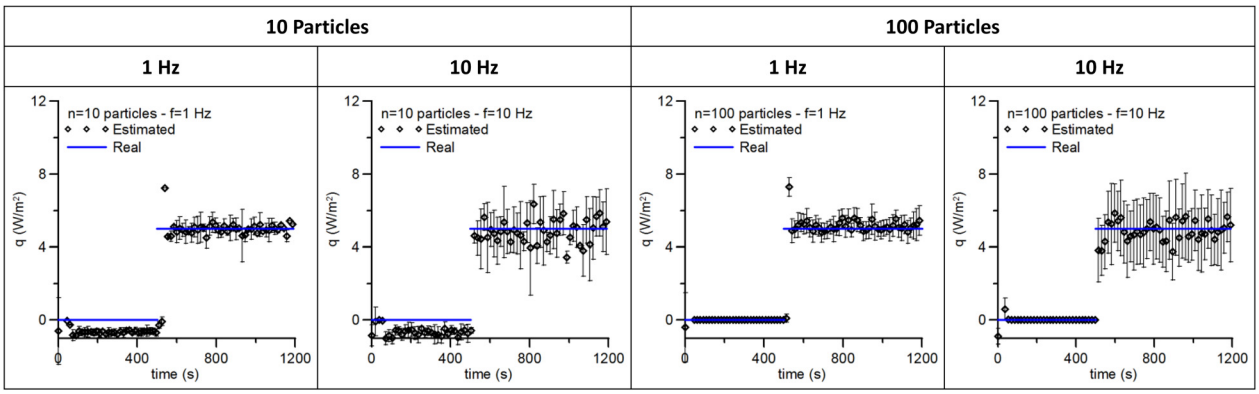

Fig. 6 Estimated heat flux with the step profile using different grids to generate the measurements and to the solution of the inverse problem (ASIR filter)

analyzed. For all test cases, the initial state for the heat flux was Gaussian, with mean equal to zero and a unity standard deviation.

Initially, the results for the scarce grid will be presented to compare both filters. At the end, results with a fully converged grid for the measurements and a scarce grid for the inverse problems will be shown for the best filter.

Figure 2 shows the estimated values of $q_2(t)$ with the linear profile (test cases 1–4) using the SIR and ASIR filters. The average values at each time are shown by the symbols with error bars corresponding to a 99% confidence interval.

For the case with 10 particles and a measurement frequency equal to 1 Hz, there was an initial delay on both filters of almost 200 s in the estimation of such heat flux. However, when the number of particles was increased to 100, with the same measurement rate of 1 Hz, both particle filters were able to fully recover the unknown heat flux. From the analysis of Fig. 2, however, it can be verified that the results for the ASIR filter present less deviation to the exact heat flux than the results obtained by the SIR filter.

When more particles were used, the error bars were more uniform during the time periods analyzed, whereas for 10 particles there was a fluctuation in the error bars as can be seen in Fig. 2. One interesting result has to do with the frequency of measurements. From Fig. 2, one can see that when the frequency was increased from 1 Hz to 10 Hz the results became

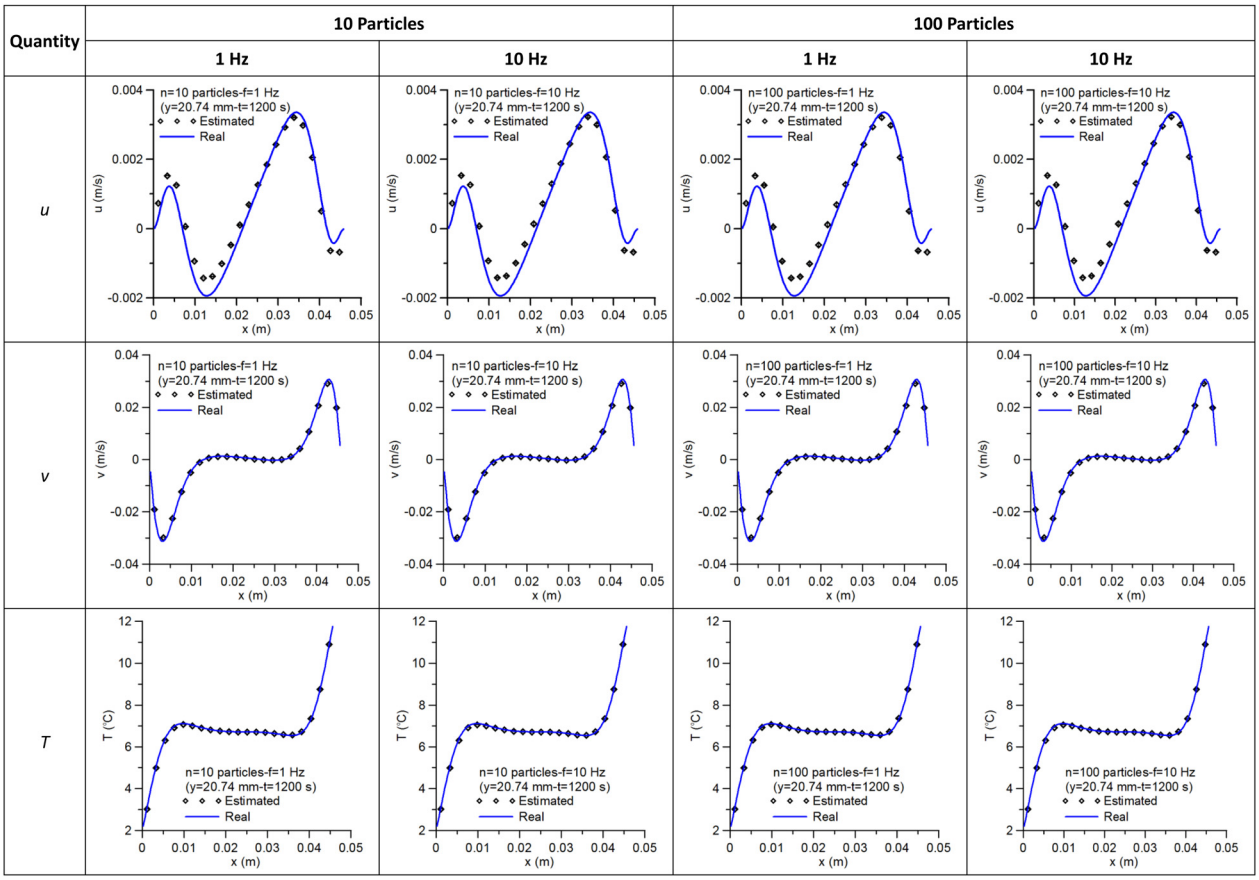

Fig. 7 Estimated *u*, *v*, and *T* with the step profile using different grids to generate the measurements and to the solution of the inverse problem (ASIR filter)

worse, with a large fluctuation of the average heat flux and larger values of the error bars. Although this has to be further investigated, we note that higher frequencies amplify the errors, while lower frequencies tend to smooth them out. The SIR filter presented a very large delay for the case with 10 particles and a frequency of measurements equal to 10 Hz, taking almost 600 s to start recovering the unknown heat flux. This initial delay was not verified in the ASIR filter and, for this reason, only results for this filter will be presented for temperature profiles and streamlines.

Figure 3 shows the real and recovered temperature profiles, while Fig. 4 shows the real and recovered streamlines, obtained by the ASIR filter, where one can notice the excellent estimates of the temperature and velocity fields. From Fig. 4, one can see that the streamlines at 100 s for the test case with 10 particles and a measurement frequency equals to 1 Hz were not very well captured, since the filter presented an initial delay of approximately 200 s to estimate such heat flux as discussed previously.

Figure 5 shows the estimated heat flux with the step profile (test cases 5–8) obtained by the particle filter methodology. Again, for 10 particles with a measurement rate equal to 1 Hz there was a delay to estimate the discontinuity at 500 s. When the number or particles was increased to 100, such delay was decreased. Also, the spread of the average value of the heat flux was less pronounced when more particles (100 instead of 10) were used. Once again, the error bars increased when the frequency of the measurement increased from 1 Hz to 10 Hz. It can also be observed that the deviation of the estimated results, compared to the exact ones, is lower for the ASIR filter, when compared to the SIR filter.

Once the superiority of the ASIR filter was demonstrated, a final result is presented, where we used a fully converged grid, with 110×110 finite volumes, to generate the measurements. Those measurements were also subjected to an experimental error with standard deviation equal to 1% of the local value of the temperature. Also, in order to explore the sensitivity of the particle filter with respect to the number of state variables, a grid with 21×21 volumes was used to the inverse problem, thus increasing the number of state variables from 364 to 1324, as discussed above. Since the grid points of those two grids were not the same, an additional error was present due to the position of the sensors. Table 4 presents the locations of the sensors for both grids. For this test case, we used the same step profile used in test cases 5–8. From Table 4, it can be seen that an average error or 1.64% is included in the location of the sensors.

Figure 6 shows the exact and estimated heat flux profiles for the test cases 9–12 using different grids for the direct and inverse problems. It can be seen that the results are remarkably good and very similar to the ones obtained for test cases 5–8, where the same grid was used for both problems. Only for the cases with 10 particles, some deviations were observed in the lower value of the heat flux. However, when the number of particles was increased, the estimate was very good. Also, even for a small number of particles, the discontinuity in the function was very well captured, showing that the ASIR filter is a very powerful inverse technique tool, even in the presence of several source of errors.

Figure 7 shows the estimated values of the u and v components of the velocity field, as well as the temperature close to the half height of the cavity for the final time. Since there was no grid points located exactly at half height of the cavity, the closest points were taken. It can be verified that in spite of some deviations for the u component of the velocity field (which has a very low value compared with v and T), the other two quantities agree very well with the real ones. It is worthwhile to mention that the real values were obtained by using a grid with 111×111 volumes, while the estimated ones came from a grid with only 21×21 volumes.

Conclusions

In this paper, we applied the SIR and the ASIR algorithms to the estimate of an unknown heat flux at the top wall of a square cavity undergoing a natural convection process. Two different heat flux profiles were estimated with very good results. Also, the number of particles as well as the frequency of the measurements were analyzed, showing that as the frequency decreases, the results improve, with lower error bars. Also, when the number of particles increases, the results become less spread around the exact value of the unknown heat flux. Numerical experiments revealed that a drastic reduction on the number of particles used to represent the posterior density function could be achieved by using the ASIR algorithm instead of the SIR algorithm. Results were also shown for cases where different grid sizes were used for the direct and inverse problems. In this test case, besides the experimental errors included in the temperatures, an additional source of error was considered, due to the fact that the measurement points were not at the same locations for the two grids. Even in this case, the ASIR algorithm was capable to recover the unknown heat flux, as well as the velocity and temperature profiles. Therefore, the ASIR algorithm appears as a robust and efficient tool for complicated state estimation problems, such as the one dealing with natural convection examined above.

Acknowledgment

The authors would like to thank the Brazilian agencies for the fostering of science, Conselho Nacional de Desenvolvimento Científico e Tecnológico (CNPq), Coordenação de Aperfeiçoamento de Pessoal de Nível Superior (CAPES), and Fundação Carlos Chagas Filho de Amparo à Pesquisa do Estado do Rio de Janeiro (FAPERJ), for the financial support for this work.

Nomenclature

C_p = specific heat at constant pressure
g = acceleration of the gravity
H = height of the cavity
k = thermal conductivity
$\mathbf{n}$ = measurement noise vector
p = pressure
q = heat flux
t = time
T = temperature
T_c = "cold" temperature
T_h = "hot" temperature
T_{ref} = reference temperature
u, v = velocity vector components in the x and y directions
$\mathbf{v}$ = state noise vector
w = weights used in the posterior density function
x, y = Cartesian coordinates
$\mathbf{x}$ = state variable vector
$\mathbf{z}$ = observation vector
β = thermal expansion coefficient
μ = molecular viscosity
ρ = density

References

[1] Kaipio, J., and Somersalo, E., 2004, *Statistical and Computational Inverse Problems* (Applied Mathematical Sciences, Vol. 160), Springer-Verlag, Berlin.
[2] Maybeck, P., 1979, *Stochastic Models, Estimation and Control*, Academic Press, New York.
[3] Winkler, R., 2003, *An Introduction to Bayesian Inference and Decision*, Probabilistic Publishing, Gainsville, FL.
[4] Kaipio, J., Duncan, S., Seppanen, A., Somersalo, E., and Voutilainen, A., 2005, "State Estimation for Process Imaging," *Handbook of Process Imaging for Automatic Control*, D. Scott and H. McCann, eds., CRC Press, Boca Raton, FL.
[5] Kalman, R., 1960, "A New Approach to Linear Filtering and Prediction Problems," ASME J. Basic Eng., **82**, pp. 35–45.
[6] Sorenson, H., 1970, "Least-Squares Estimation: From Gauss to Kalman," IEEE Spectrum, **7**, pp. 63–68.
[7] Welch, G., and Bishop, G., 2006, *An Introduction to the Kalman Filter*, UNC, Chapel Hill, Report No. TR 95-041.
[8] Arulampalam, S., Maskell, S., Gordon, N., and Clapp, T., 2001, "A Tutorial on Particle Filters for On-Line Non-Linear/Non-Gaussian Bayesian Tracking," IEEE Trans. Signal Process., **50**, pp. 174–188.

[9] Ristic, B., Arulampalam, S., and Gordon, N., 2004, *Beyond the Kalman Filter*, Artech House, Boston.
[10] Doucet, A., Godsill, S., and Andrieu, C., 2000, "On Sequential Monte Carlo Sampling Methods for Bayesian Filtering," Stat. Comput., **10**, pp. 197–208.
[11] Liu, J., and Chen, R., 1998, "Sequential Monte Carlo Methods for Dynamical Systems," J. Am. Stat. Assoc., **93**, pp. 1032–1044.
[12] Andrieu, C., Doucet, A., and Robert, C., 2004, "Computational Advances for and From Bayesian Analysis," Stat. Sci., **19**, pp. 118–127.
[13] Johansen, A., and Doucet, A., 2008, "A Note on Auxiliary Particle Filters," Stat. Probab. Lett., **78**(12), pp. 1498–1504.
[14] Carpenter, J., Clifford, P., and Fearnhead, P., 1999, "An Improved Particle Filter for Non-Linear Problems," IEE Proc., Radar Sonar Navig., **146**, pp. 2–7.
[15] Del Moral, P., Doucet, A., and Jasra, A., 2007, "Sequential Monte Carlo for Bayesian Computation," *Bayesian Statistics*, Vol. 8, Oxford University Press, Cary, North Carolina, pp. 1–34.
[16] Del Moral, P., Doucet, A., and Jasra, A., 2006, "Sequential Monte Carlo Samplers," J. R. Stat. Soc., **68**, pp. 411–436.
[17] Andrieu, C., Doucet, A., Singh, S. S., and Tadic, V. B., 2004, "Particle Methods for Charge Detection, System Identification and Control," Proc. IEEE, **92**, pp. 423–438.
[18] Hammersley, J. M., and Hanscomb, D. C., 1964, *Monte Carlo Methods*, Chapman and Hall, London.
[19] Gordon, N., Salmond, D., and Smith, A. F. M., 1993, "Novel Approach to Nonlinear and Non-Gaussian Bayesian State Estimation," IEE Proc. F, Radar Signal Process., **140**, pp. 107–113.
[20] Orlande, H., Dulikravich, G., and Colaço, M., 2008, "Application of Bayesian Filters to Heat Conduction Problem," *EngOpt 2008—International Conference on Engineering Optimization*, J. Herskovitz, ed., Rio de Janeiro, Brazil, June 1–5.
[21] Pitt, M., and Shephard, N., 1999, "Filtering via Simulation: Auxiliary Particle Filters," J. Am. Stat. Assoc., **94**(446), pp. 590–599.
[22] Liu, J., and West, M., 2001, "Combined Parameter and State Estimation in Simulation-Based Filtering," *Sequential Monte Carlo Methods in Practice*, A. Doucet, N. de Freitas, and N. Gordon, eds., Springer-Verlag, New York, pp. 197–217.
[23] West, M., 1993, "Approximating Posterior Distributions by Mixture," J. R. Stat. Soc. Ser. B (Methodol.), **55**, pp. 409–422. Available at: http://www.jstor.org/stable/2346202.
[24] Sisson, S. A., Fan, Y., and Tanaka, M. M., 2009, "Sequential Monte Carlo Without Likelihoods," Proc. Natl. Acad. Sci. U.S.A., **104**, pp. 1760–1765, Errata, 2007.
[25] Batchelor, G. K., 2000, *An Introduction to Fluid Dynamics*, Cambridge University Press, Cambridge.
[26] Versteeg, H., and Malalasekera, W., 2007, *An Introduction to Computational Fluid Dynamics: The Finite Volume Method*, Prentice-Hall, Englewood Cliffs, NJ.
[27] Van Doormal, J. P., and Raithby, G. D., 1984, "Enhancements of the SIMPLE Method for Predicting Incompressible Fluid Flow," Numer. Heat Transfer, **7**, pp. 147–163.
[28] Raithby, G. D., and Torrance, K. E., 1974, "Upstream-Weighted Differencing Schemes and Their Application to Elliptic Problems Involving Fluid Flow," Comput. Fluids, **2**, pp. 191–206.
[29] Saad, Y., and Schultz, M., 1985, "Conjugate Gradient-Like Algorithms for Solving Non-Symmetric Linear Systems," Math. Comput., **44**(170), pp. 417–424.
[30] Colaço, M. J., and Orlande, H. R. B, 1999, "A Comparison of Different Versions of the Conjugate Gradient Method of Function Estimation," Numer. Heat Transfer, Part A, **36**(2), pp. 229–249.
[31] Colaço, M. J., and Orlande, H. R. B, 2001, "Inverse Problem of Simultaneous Estimation of Two Boundary Heat Fluxes in Parallel Plate Channels," J. Braz. Soc. Mech. Eng., **23**(2), pp. 201–215.
[32] Colaço, M. J., and Orlande, H. R. B, 2001, "Inverse Forced Convection Problem of Simultaneous Estimation of Two Boundary Heat Fluxes in Irregularly Shaped Channels," Numer. Heat Transfer, Part A, **39**, pp. 737–760.
[33] Colaço, M. J., Dulikravich, G. S., and Martin, T. J., 2004, "Optimization of Wall Electrodes for Electro-Hydrodynamic Control of Natural Convection During Solidification," Mater. Manuf. Processes, **19**(4), pp. 719–736.
[34] Colaço, M. J., and Orlande, H. R. B, 2004, "Inverse Natural Convection Problem of Simultaneous Estimation of Two Boundary Heat Fluxes in Irregular Cavities," Int. J. Heat Mass Transfer, **47**, pp. 1201–1215.
[35] Colaço, M. J., Dulikravich, G. S., and Martin, T. J., 2005, "Control of Unsteady Solidification via Optimized Magnetic Fields," Mater. Manuf. Processes, **20**(3), pp. 435–458.
[36] Colaço, M. J., and Dulikravich, G. S., 2006, "A Multilevel Hybrid Optimization of Magnetohydrodynamic Problems in Double-Diffusive Fluid Flow," J. Phys. Chem. Solids, **67**, pp. 1965–1972.
[37] Colaço, M. J., and Dulikravich, G. S., 2007, "Solidification of Double-Diffusive Flows Using Thermo-Magneto-Hydrodynamics and Optimization," Mater. Manuf. Processes, **22**, pp. 594–606.
[38] Beck, J. V., and Arnold, K. J., 1977, *Parameter Estimation in Engineering and Science*, Wiley Interscience, New York.
[39] Calvetti, D., and Somersalo, E., 2007, *Introduction to Bayesian Scientific Computing*, Springer, New York.
[40] Tan, S., Fox, C., and Nicholls, G., 2006, *Inverse Problems* (Course Notes for Physics 707), University of Auckland, Auckland, New Zealand.
[41] Lee, P. M., 2004, *Bayesian Statistics*, Oxford University Press, London.
[42] Gamerman, D., and Lopes, H. F., 2006, *Markov Chain Monte Carlo: Stochastic Simulation for Bayesian Inference*, 2nd ed., Chapman and Hall/CRC, Boca Raton, FL.
[43] Wang, J., and Zabaras, N., 2004, "A Bayesian Inference Approach to the Stochastic Inverse Heat Conduction Problem," Int. J. Heat Mass Transfer, **47**, pp. 3927–3941.
[44] Wang, J., and Zabaras, N., 2004, "A Computational Statistics Approach to Stochastic Inverse Problems and Uncertainty Quantification in Heat Transfer," Proceedings of the VI World Conference on Computational Mechanics, Beijing, China, Sept. 5–10.
[45] Mota, C. A. A., Orlande, H. R. B., Wellele, O., Kolehmainen, V., and Kaipio, J., 2009, "Inverse Problem of Simultaneous Identification of Thermophysical Properties and Boundary Heat Flux," High Temp. – High Press., **38**, pp. 171–185.
[46] Orlande, H. R. B., Kolehmainen, V., and Kaipio, J. P., 2007, "Reconstruction of Thermal Parameters Using a Tomographic Approach," Int. J. Heat Mass Transfer, **50**, pp. 5150–5160.
[47] Emery, A. F., 2007, "Estimating Deterministic Parameters by Bayesian Inference With Emphasis on Estimating the Uncertainty of the Parameters," *Proceedings of the Inverse Problem, Design and Optimization Symposium*, G. Dulikravich, H. Orlande, and M. Colaco, eds., Miami Beach, FL, Vol. 1, pp. 266–272.
[48] Mota, C., Orlande, H., De Carvalho, M., Kolehmainen, V., and Kaipio, J., 2010, "Bayesian Estimation of Temperature-Dependent Thermophysical Properties and Transient Boundary Heat Flux," Heat Transfer Eng., **31**, pp. 570–580.
[49] Naveira-Cotta, C., Orlande, H., and Cotta, R., 2010, "Integral Transforms and Bayesian Inference in the Identification of Variable Thermal Conductivity in Two-Phase Dispersed Systems," Numer. Heat Transfer, **57**, pp.173–202.
[50] Naveira-Cotta, C., Cotta, R., and Orlande, H., 2010, "Inverse Analysis of Forced Convection in Micro-Channels With Slip Flow via Integral Transforms and Bayesian Inference," Int. J. Therm. Sci., **49**, pp. 879–888.
[51] Naveira-Cotta, C., Orlande, H., Cotta, R., and Nunes, J., 2010, "Integral Transforms, Bayesian Inference, and Infrared Thermography in the Simultaneous Identification of Variable Thermal Conductivity and Diffusivity in Heterogeneous Media," Proceedings of the International Heat Transfer Conference IHTC14, Washington, DC, Aug. 8–13, Paper No. IHTC14-22511.
[52] Fudym, O., Orlande, H. R. B., Bamford, M., and Batsale, J. C., 2008, "Bayesian Approach for Thermal Diffusivity Mapping From Infrared Images With Spatially Random Heat Pulse Heating," J. Phys.: Conf. Ser., **135**, pp. 12–42.
[53] Massard, H., Fudym, O., Orlande, H. R. B., and Batsale, J. C., 2010, "Nodal Predictive Error Model and Bayesian Approach for Thermal Diffusivity and Heat Source Mapping," C. R. Méc., **338**, pp. 434–449.
[54] Orlande, H., Colaço, M., and Dulikravich, G., 2008, "Approximation of the Likelihood Function in the Bayesian Technique for the Solution of Inverse Problems," Inverse Probl. Sci. Eng., **16**(6), pp. 677–692.
[55] Parthasarathy, S., and Balaji, C., 2008, "Estimation of Parameters in Multi-Mode Heat Transfer Problems Using Bayesian Inference—Effect of Noise and *a priori*," Int. J. Heat Mass Transfer, **51**, pp. 2313–2334.
[56] Kaipio, J., and Fox, C., "The Bayesian Framework for Inverse Problems in Heat Transfer," Heat Transfer Eng., **32**(9), pp. 718–753.
[57] Godsill, S., Doucet, A., and West, M., 2004, "Monte Carlo Smoothing for Nonlinear Time Series," J. Am. Stat. Assoc., **99**, pp. 156–168.
[58] Doucet, A., Freitas, N., and Gordon, N., 2001, *Sequential Monte Carlo Methods in Practice*, Springer, New York.